

Integrative visualization of the molecular structure of a cellular microdomain

David S. Goodsell^{1,2,3,4}  | Keren Lasker¹ 

¹Department of Integrative Structural and Computational Biology, The Scripps Research Institute, La Jolla, California, USA

²Research Collaboratory for Structural Bioinformatics Protein Data Bank, Rutgers, The State University of New Jersey, Piscataway, New Jersey, USA

³Institute for Quantitative Biomedicine, Rutgers, The State University of New Jersey, Piscataway, New Jersey, USA

⁴Rutgers Cancer Institute of New Jersey, Rutgers, The State University of New Jersey, New Brunswick, New Jersey, USA

Correspondence

David S. Goodsell and Keren Lasker,
Department of Integrative Structural and
Computational Biology, The Scripps
Research Institute, 10550 N. Torrey Pines
Road, La Jolla, CA 92037, USA.
Email: goodsell@scripps.edu and
klasker@scripps.edu

Funding information

National Institutes of Health,
Grant/Award Numbers: GM120604,
GM133198; National Science Foundation,
Grant/Award Number: DBI-1832184;
U.S. Department of Energy, Grant/Award
Number: DE-SC0019749

Review Editor: John Kuriyan

Abstract

An integrative approach to visualization is used to create a visual snapshot of the structural biology of the polar microdomain of *Caulobacter crescentus*. The visualization is based on the current state of molecular and cellular knowledge of the microdomain and its cellular context. The collaborative process of researching and executing the visualization has identified aspects that are well determined and areas that require further study. The visualization is useful for dissemination, education, and outreach, and the study lays the groundwork for future 3D modeling and simulation of this well-studied example of a cellular condensate.

KEYWORDS

Caulobacter crescentus, cellular condensate, integrative structural biology, intrinsically disordered protein, molecular visualization, PopZ

1 | INTRODUCTION

The aquatic bacterium *Caulobacter crescentus* has emerged as a simple model organism for study of cellular development and differentiation (Curtis & Brun, 2010; Govers & Jacobs-Wagner, 2020; Lasker et al., 2016; Tsokos & Laub, 2012). It has a two-step life cycle, born as a DNA replication-incompetent free-swimming “swarmer” and differentiating into a DNA replication-competent immobile “stalked” cell. As part of this process, the cell populates the two ends of the cell (poles) with scaffolding and signaling proteins that regulate these two distinct life forms (Figure 1, left). These specialized polar complexes guide construction

of flagellar motors and pili in the swarmer form and the shedding of the flagellum, retraction of the pili, and construction of a stalk with an adhesive tip (hold-fast) in the stalked form (Ardisson & Viollier, 2015; Mignolet et al., 2018). Critically, these complexes regulate signaling pathways that activate replication and segregation of the DNA chromosome exclusively in stalked cells (Frandi & Collier, 2019).

How are these signaling proteins localized to the pole and how is the composition of the polar region maintained? These polar regions are defined by self-assembly of the polar organizing protein Z (PopZ) that marks a specific microdomain at the poles, selectively gathers scaffolding and signaling macromolecular

This is an open access article under the terms of the [Creative Commons Attribution](https://creativecommons.org/licenses/by/4.0/) License, which permits use, distribution and reproduction in any medium, provided the original work is properly cited.

© 2023 The Authors. *Protein Science* published by Wiley Periodicals LLC on behalf of The Protein Society.

complexes (“client” proteins), and excludes large cytoplasmic molecules like ribosomes as well as smaller proteins that do not bind to members of the microdomain (Bowman et al., 2008, 2010; Ebersbach et al., 2008; Gahlmann et al., 2013; Holmes et al., 2016; Lasker et al., 2020). In this illustration (Figure 1, right), we capture the current knowledge about the composition and structure of the PopZ microdomain at the flagellated pole. In particular, we highlight the role PopZ plays in bringing these signaling proteins together. Below, we provide a brief overview of the main components of this illustration, namely PopZ and the clients that reside within this microdomain.

1.1 | PopZ, clients, and the polar microdomain

PopZ shows many of the characteristic features shared by molecules that form cellular condensates (Banani et al., 2017; Nordyke et al., 2020; Posey et al., 2018; Ptacin et al., 2014; Shin & Brangwynne, 2017). PopZ is largely disordered. Its N-terminal region binds clients through a short conserved helix (Holmes et al., 2016; Nordyke et al., 2020). The central region of PopZ is disordered with many prolines and negatively charged amino acids and likely acts as a tuner of PopZ material properties (Lasker et al., 2022). Self-assembly is mediated by

interactions between three helices at the C-terminal helical region (Figure 2a,b; Bowman et al., 2010; Bowman et al., 2013; Laloux & Jacobs-Wagner, 2013; Lasker et al., 2022). In our current model, based on biochemical and structural data, PopZ associates into trimers and hexamers decorated with long intrinsically disordered regions (IDRs), with client-interacting helices at their tips (manuscript in preparation). The hexamers are likely to further associate into filaments, as observed in cryoelectron micrographs (Toro-Nahuelpan et al., 2022; Figure 2c,d).

The PopZ condensate recruits multiple client proteins that mediate pole-specific functions in the cell. Currently known clients are enumerated in Table 1, and include cytosolic regulatory proteins and a diverse collection of membrane-bound histidine kinases, scaffolding proteins, and proteins that mediate formation of the flagellar motor and pili. Clients that are specific to the stalk pole are not included in this list.

1.2 | Regulatory cascades

The two-component signaling protein CtrA is the main regulator of *Caulobacter* asymmetry through its dual roles as an inhibitor of DNA replication initiation and as a transcription factor that controls expression of many genes involved in swarmer cell fate (Laub et al., 2002; Quon et al., 1998). Unlike other transcriptional regulators in *Caulobacter*, CtrA must be phosphorylated (CtrA~P) to be active as a transcription factor (Domian et al., 1997).

CtrA levels and its phosphorylation state are regulated by signaling cascades that happen primarily at the poles, which implement either a CtrA activation or CtrA degradation cascade depending on cell-cycle state (Zik & Ryan, 2022). Upon compartmentalization of the predivisional cell, CtrA drives asymmetry by remaining phosphorylated and active in the swarmer compartment while being dephosphorylated and degraded in the stalked compartment (Tsokos & Laub, 2012).

The phosphorylation state and levels of CtrA are determined by the bifunctional hybrid histidine kinase CckA (Jacobs et al., 1999). When stimulated as a kinase, CckA autophosphorylates and transfers its phosphate to the phosphotransfer protein ChpT (Biondi et al., 2006; Blair et al., 2013; Chen et al., 2009), which in turn passes the phosphate to either CtrA, resulting in its activation, or to CpdR, resulting in inhibition of CtrA degradation (Iniesta & Shapiro, 2008). When CckA is stimulated as a phosphatase, phosphoryl groups are transferred back from CtrA through ChpT to CckA, where they are hydrolyzed (Biondi et al., 2006). This reverse process inhibits the activation of CtrA and promotes CtrA degradation by shutting off the flow of phosphate to CpdR. The dual functions of CckA act

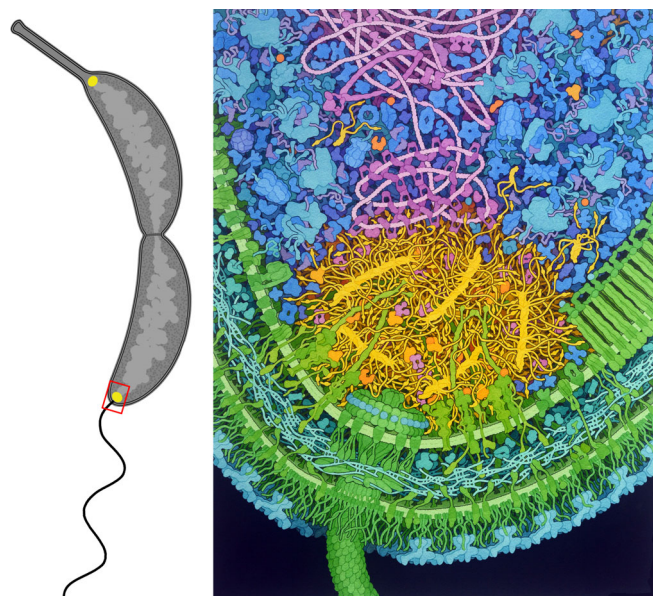


FIGURE 1 Illustration of a predivision *Caulobacter* cell (left) with the sessile daughter cell at the top and the swarmer daughter cell at the bottom. Close-up of the flagellated pole (right), with the PopZ in yellow, soluble clients in orange, cytoplasm in blue and purple, nucleoid in magenta, and cell wall in green and turquoise.

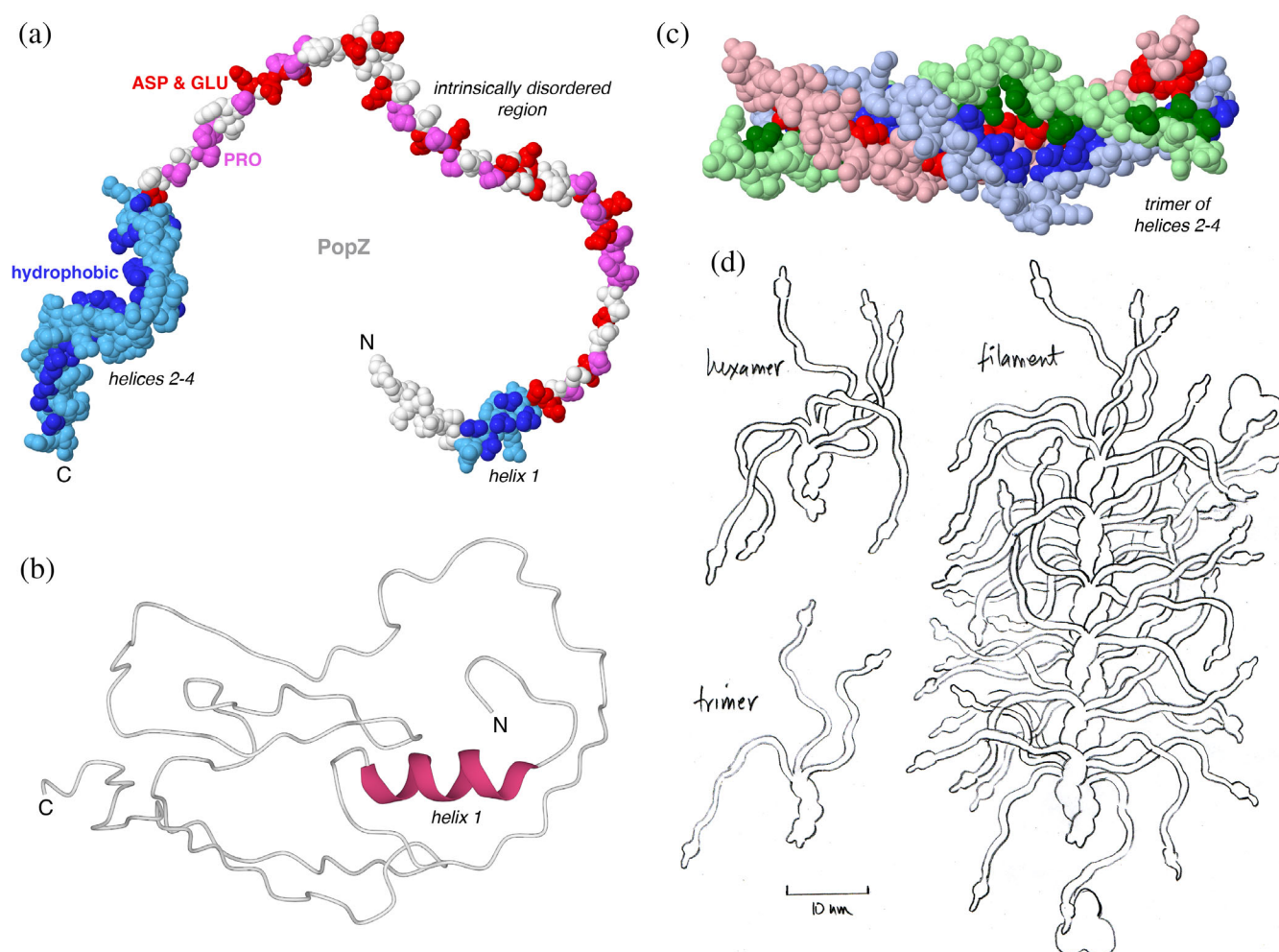


FIGURE 2 PopZ structures and models. (a) Model of the PopZ monomer as predicted by AlphaFold2 (top) contains a short N-terminal helix (blue), an IDR rich in proline (magenta) and negatively charged amino acids (red), and three closely spaced helices at the C-terminus (blue). The helices are amphipathic, as illustrated by coloring hydrophobic amino acids a darker shade of blue. The N-terminal helix interacts with client proteins and the C-terminal helices mediate oligomerization. Coordinates for PopZ from AF-Q9A8N4-F1-model_v3, with modified torsion angles at residue 73 to give a more extended structure for this figure. (b) Structure of PopZ 1–133 determined by NMR, from PDB ID 6xry, colored by secondary structure with alpha helices in magenta and disordered regions in white. (c) Trimer model of C-terminal region predicted using AlphaFold2 (manuscript in preparation). (d) Sketch of PopZ trimer, hexamer, and filament based on these structures, created during the collaborative dialog between the authors.

as a switch that leads to either CtrA activation, to promote swarmer fate, or CtrA degradation, to promote stalk fate.

CckA state is in turn regulated by the composition of the pole it resides in. Accumulation of CckA at the flagellated cell pole is mediated by the pseudokinase DivL and promotes kinase activity in the swarmer compartment (Iniesta & Shapiro, 2008; Mann & Shapiro, 2018; Mann et al., 2016). In addition, the phosphorylation state of two response regulators, DivK and PleD (Hecht et al., 1995; Hecht & Newton, 1995) modulate CckA state. DivK, when phosphorylated, binds to DivL, and this DivL-DivK~P complex can inhibit CckA kinase activity (Childers et al., 2014; Tsokos et al., 2011). PleD, when phosphorylated, synthesizes cyclic-di-GMP (cdG), which can bind CckA and

inhibit its kinase activity (Lori et al., 2015; Mann et al., 2016). The levels of DivK~P and PleD~P are modulated by the swarmer fate determinant PleC, which is localized to the flagellated pole and the stalked fate determinant DivJ, which is localized to the stalk cell pole. PleC dephosphorylates DivK~P and PleD~P, permitting the activity of CckA in the swarmer compartment (Abel et al., 2013; Christen et al., 2010; Lam et al., 2003; Wheeler & Shapiro, 1999). Thus, CckA integrates information about the progression of assembly of the CtrA activation pathway and of cellular compartmentalization to regulate the phosphorylation state and stability of CtrA.

The AAA+ protease ClpXP degrades CtrA in a cell cycle-dependent manner (Fatima et al., 2022; Joshi & Chien, 2016;

TABLE 1 Molecular oligomerization and abundances.

Protein	Assembly	Number/ cell ^a	Fraction ^b	Number/ foreground ^c	Reference
PopZ	6	8200	0.5	28.5	(Bowman et al., 2008; Ebersbach et al., 2008)
Membrane clients					
Podj	2	700	0.9	8.8	(Hinz et al., 2003; Viollier et al., 2002)
PleC	2	688	0.8	7.6	(Jacobs et al., 2001)
DivL	2	589	0.6	4.9	(Tsokos et al., 2011)
CckA	2, 4 ^d	734	0.8	8.2	(Angelastro et al., 2010)
ZitP	1	617	0.9	15.4	(Bergé et al., 2016)
Soluble clients					
ChpT	2	1493	0.2	6.2	(Guzzo et al., 2021; Lasker et al., 2020)
CtrA	2	25,402	0.03	15.9	(Lasker et al., 2020; Ryan et al., 2004)
CpdR	1	6044	0.01	2.5	(Iniesta et al., 2006)
RcdA	2	2583	0.03	1.6	(McGrath et al., 2006)
ParB	2	2072	0.45	19.4	(Jalal & Le, 2020; Ptacin et al., 2014)
DivK	1	2671	0.03	3.3	(Matroule et al., 2004)
PleD	2	1359	0.03	0.8	(Paul et al., 2004)
PopA	1	930	0.3	11.6	(Duerig et al., 2009; Wang et al., 2021)

^aNumber of protein chains per cell.^bFraction of molecules located at the pole.^cNumber of assemblies to be included in the foreground layer of the painting. See text for calculation.^dMay assemble into tetramers, as shown in the illustration.

Schroeder & Jonas, 2021). CpdR, RcdA, and the cdG receptor PopA are required for degradation of CtrA by ClpXP when bound to the chromosome. The signaling proteins inside the polar region coordinate the availability of these three adaptors, in a hierarchical manner, to bind ClpXP at the right time and place (Gora et al., 2013; Joshi et al., 2015; Smith et al., 2014).

1.3 | ParB and DNA segregation

The ParABS system is an active DNA segregation system that was first identified to play a role in the stable inheritance of low-copy-number plasmids (Abeles et al., 1985; Austin & Abeles, 1983; Mori et al., 1986). In addition to plasmids, numerous bacterial species use ParABS to segregate their chromosomes (Livny et al., 2007), including *C. crescentus* (Mohl et al., 2008; Ptacin et al., 2010). The ParABS system consists of three conserved components: the origin-proximal centromeric DNA sequence, *parS*; the CTPase ParB, which binds *parS*, spreads, and nucleates a nucleoprotein complex on a *parS* sequence (Antar et al., 2021; Böhm et al., 2020; Breier & Grossman, 2007; Lagage et al., 2016), and the Walker-box ATPase ParA, which interacts with ParB and drives the segregation of the ParB-DNA nucleoprotein complex to partition replicated

chromosomes to each daughter cell (Easter & Gober, 2002; Leonard et al., 2005). In *Caulobacter*, PopZ anchors the ParB-*parS* complex to the cell poles through direct interaction with ParB (Bowman et al., 2008). PopZ also binds ParA, and sequestration of ParA into PopZ stimulates recycling of ParA into a nucleoid-bound complex to ensure pole-specific centromere transfer (Bowman et al., 2008; Laloux & Jacobs-Wagner, 2013; Ptacin et al., 2014).

1.4 | Integrative visualization

This work is based on the hypothesis: “Can we create a visualization that shows a portion of this cell, including all macromolecules and based on the current state of structural, bioinformatic, biochemical, and micrographic knowledge?” We have taken a two-pronged approach to address this hypothesis in other systems. First, we have used traditional scientific illustration methods to create depictions of cross-sections through many types of cells, primarily for use in scientific dissemination, education, and outreach (Goodsell, 1991, 2021). Second, when technically possible, we have created 3D computational models of these cells, for example, in recent models of whole mycoplasma and minimal genome cells (Goodsell, 2022; Maritan et al., 2022). Increasingly, we are using the

illustration effort as a prelude to full 3D modeling, as a tool to enumerate the many types of structures and interactions that need to be modeled. This report presents the first step in this process for the *Caulobacter* flagellar polar region, gathering and curating the necessary information and integrating it to create an illustrative snapshot of the cell that captures the current state of knowledge (Figure 1).

2 | RESULTS

2.1 | Overview of illustration

The illustration depicts the flagellar pole of a *Caulobacter crescentus* predivisional cell, centered on the PopZ microdomain. Each PopZ filament comprised of 5–7 hexamers, with many IDR extending from a central helical core. Helix 1 is shown as a small globule near the end of each IDR. Membrane-bound and soluble clients are embedded in the PopZ matrix, primarily interacting with Helix 1, and several free soluble clients are shown in the adjacent cytoplasm, along with free PopZ trimers and hexamers. The nucleoid interacts with PopZ through the client protein ParB, which is shown condensing on a short region of the DNA through spreading of closed forms and bridging of open forms (Jalal & Le, 2020). Also shown on the chromosome are the DNA-binding proteins SMC (Jensen & Shapiro, 1999; Tran et al., 2017) and GapR (Guo et al., 2018) as well as the master transcription factor CtrA bound to five sites near the chromosomal origin of replication. Other features specific to the flagellated pole include a flagellar motor and chemosensory array.

2.2 | Sources and confidence

Diverse sources of data were gathered, curated, and integrated into the illustration, as described in detail in the Methods. The ultrastructure is based on cryoelectron tomography and fluorescence microscopy, which is sufficient to define the geometry of the cell wall and chemosensory array, positions of individual ribosomes, and volume of the microdomain (Dahlberg et al., 2020; Gahlmann et al., 2013; Lasker et al., 2020). The flagellar motor is not present in the source micrographs, and was added based on separate single-particle cryoEM studies (Rossmann et al., 2020). Structures for individual molecules were gathered from multiple sources, leveraging the effective search methods available at UniProt (uniprot.org) and RCSB PDB (rcsb.org). These include experimental structures of *Caulobacter* proteins and proteins from related organisms, homology models, and

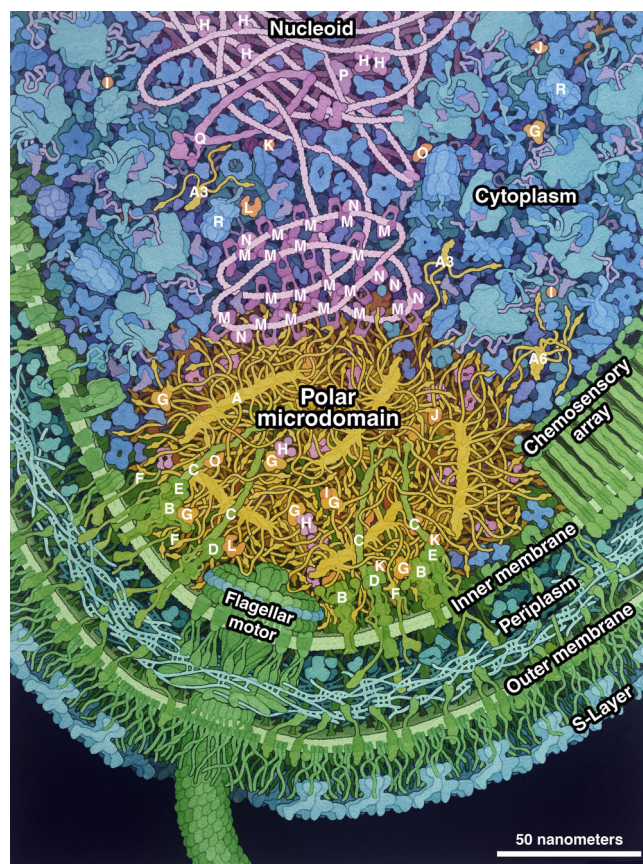


FIGURE 3 Key to the illustration. PopZ: A, PopZ microfilament; A6, PopZ hexamer; A3, PopZ trimer. Clients: B, CckA; C, PodJ; D, PleC; E, DivL; F, ZitP; G, ChpT; H, CtrA; I, CpdR; J, RdcA; K, DivK; L, PleD; M, ParB; N, MipZ; O, PopA; P, ParA. Proteins related to the microdomain: Q, SMC (structural maintenance of chromosomes); R, ClpXP.

predicted structures from AlphaFold2 (Jumper et al., 2021). Individual proteins related to the microdomain are identified in Figure 3.

Abundances are based on data from ribosome profiling (Schrader et al., 2016). The fraction of each protein found at the pole is determined based on relative fluorescent levels of the protein at the pole versus the rest of the cell (Table 1). The absolute number of molecules depicted in the painting is estimated using these abundances and fractions, scaled to give an overall concentration similar to the cytoplasm. Interactions were among the most difficult types of information to find: they were determined one-by-one by searching the primary research literature and by personal communication with the community of *Caulobacter* experts (Table 2).

In these types of integrative efforts, which seek to include all macromolecules in the proper place and proper abundance, it is necessary to work with the current state of knowledge, which may be fragmentary for some aspects of the scene. The *Caulobacter* illustration heavily leverages

TABLE 2 Microdomain interactions.

Interacting	Proteins	Reference
PopZ	PodJ	(Zhao et al., 2018)
PopZ	CckA	(Holmes et al., 2016)
PopZ	ZitP	(Bergé et al., 2016)
PopZ	ChpT	(Holmes et al., 2016; Lasker et al., 2020)
PopZ	CpdR	(Holmes et al., 2016)
PopZ	RcdA	(Nordyke et al., 2020)
PopZ	ParB	(Bowman et al., 2008; Ptacin et al., 2014)
PodJ	PleC	(Zhang et al., 2022)
PodJ	DivL	(Curtis et al., 2012)
PodJ	PopA	(Curtis et al., 2012)
PleC	DivK	(Childers et al., 2014; Matroule et al., 2004)
PleC	PleD	(Aldridge et al., 2003)
DivL	CckA	(Childers et al., 2014; Tsokos et al., 2011)
DivL	DivK	(Reisinger et al., 2007; Tsokos et al., 2011)
ZitP	CpaE	(Bergé et al., 2016)
ChpT	CtrA	(Blair et al., 2013)
ChpT	CpdR	(Blair et al., 2013)
ParB	ParA	(Figge et al., 2003)
ParB	MipZ	(Figge et al., 2003)

previous work on *E. coli* for overall features of the cytoplasm and cell wall, while confirming the presence of each molecule in the *Caulobacter* genome. Strong structural data are available for the soluble clients; however, the membrane-bound clients and PopZ are all subjects of this study, so these molecules are depicted based on speculative models informed largely by predicted models from AlphaFold2 and relationships to similar well-characterized systems. Interactions between PopZ and clients are also a topic that is currently under investigation—generally, the interaction sites in PopZ are well defined, but the sites on clients less so.

2.3 | Design and rendering choices

As in previous illustrative work, the *Caulobacter* illustration employs intentional artistic license to improve the readability of the image (Goodsell, 2009, 2022). The image depicts all macromolecules using simplified shapes, all drawn in canonical views for easy recognition. Disordered molecules (PopZ IDR, mRNA, lipopolysaccharide, etc.) are rendered with slightly exaggerating chain width to improve

visibility. The entire scene depicts a cross section through the cell, rendered in orthographic projection to allow comparison of sizes across the image, and employing sharp depth cueing to separate background from foreground.

Extended features such as the PopZ filament/IDR, chromosome, and peptidoglycan network are arranged entirely in the plane of the image, so that none are clipped. This choice is made to improve comprehension of the overall structure of these features, but may induce artifacts in the details of local arrangement and interactions. For example, the five PopZ filaments are arranged flat in the foreground layer, with the IDR all extending within this narrow slab of space. Three-dimensional models of the condensate will be needed to explore more accurate arrangements of filaments within the condensate space.

Conformations of molecules are chosen to improve a high-level understanding of the scene. PopZ IDRs are depicted as long, sinuous chains that interdigitate and fill space, whereas NMR structures of individual PopZ IDRs (PDB ID 6xry) show a more compact structure. Similarly, peptidoglycan and lipopolysaccharide chains are shown as mostly extended. In all cases, this gives an impression of the length of chains in relation to other molecules in the scene. These choices underscore the need for detailed mesoscale modeling to probe their 3D conformation within this crowded environment.

Colors and composition are chosen to highlight the central story told by the illustration: the structure and function of the condensate. The color palette highlights functional compartments of the cell, with microdomain in yellow and orange, cell wall in green, cytoplasm in blue, and nucleoid in magenta. Colors of individual molecules are consistent across the illustration, so, for example, soluble client proteins (orange) may be seen in different contexts in the microdomain and in the cytoplasm. Bright, warm colors are chosen for the microdomain and clients to focus attention on them. In previous bacterial illustrations, a visually stable composition was designed with the cell wall and flagellar motor at the top, enclosing the cytoplasm and nucleoid below. A reversed composition was employed in the *Caulobacter* illustration with the cell wall and flagellar motor at the bottom, microdomain centered, and nucleoid entering the frame from the top. This less-stable composition was chosen intentionally to shift focus to the nucleoid and microdomain.

3 | DISCUSSION

3.1 | Science art collaboration

The current SciArt movement has goals as diverse as its community of scientists and artists, ranging from the free

expression inherent in fine art (Gewin, 2021; Root-Bernstein et al., 2011) to art that is conceived as a tool for scientific research and dissemination (Goodsell, 2021; Zhu & Goyal, 2019). The central goal in the work described here is to use traditional illustrative techniques to create an integrated conception of the state of the field—in this case, liquid–liquid phase separation in bacteria—for use in dissemination of results and outreach to other communities. However, the act of collaboration is arguably the most important aspect of this process. For example, this project provided the opportunity to formally gather and curate diverse information related to the molecular composition, abundance, and interactions of all components of condensate, often drawing on expert opinions from other researchers in the field. In essence, the illustration acts as a visual review of the field.

In these types of collaborations, it is important that there is a two-way dialog throughout the process. Many challenges are addressed during this dialog. For example, early in planning, we chose to depict the flagellated pole in order to avoid the additional complexity of the stalk structure. Perhaps most importantly, this type of integrative illustration requires that decisions are made for aspects that are still under study, based on current hypotheses or intuition. As such, they represent a snapshot of the current state of the subject. Table 3 outlines several aspects of the microdomain structure that are still under study and the assumptions that we made when depicting these aspects in the illustration.

In addition, the choice of design and rendering often place restrictions on what can be shown. For example, the watercolor technique used here can show a scene several hundred nanometers wide while still making the individual macromolecules recognizable. The magnification, however, makes inclusion of small molecules, ions, and water unfeasible.

3.2 | Implications to *Caulobacter* biology

This illustration provides an integrated view that for the first time integrates current knowledge into a single figure. Critical features of the domain are depicted, providing one conception of the interplay of PopZ, clients, flagellar motor, and the surrounding membrane and cytoplasm, all of which are consistent with currently available information. By doing so, the illustration provides a thinking tool for comprehension of the mesoscale properties and organization of the polar microdomain. For example, the choices made during design and rendering of the illustration pose several interesting mesoscale-level questions. How are signals from the chemotaxis array transformed to the flagella motor through the PopZ

TABLE 3 Aspects of the illustration with limited available information.

Aspects with limited information	Assumptions in the illustration
Limited structural information for membrane-bound clients	Combination of AlphaFold2 structures and UniProt annotations to depict domain structure
Site of PopZ interaction on client is not known for most clients (Table 2)	Arbitrary position chosen
Density of PopZ within condensate is not fully characterized	Condensate assigned typical concentration of prokaryotic cytoplasm
PopZ–PopZ interactions still under active study	Used trimer/hexamer/filament model from Lasker lab; additional filament/filament interactions, if they exist, not shown
Detailed confirmation of PopZ IDR within condensate not fully characterized	Assumed an extended conformation that improved clarity of the illustration
Interface of condensate with flagellar motor not characterized in detail	No specific interaction depicted
Complete composition of the PopZ microdomain is not known	Compiled a list of proteins residing within the microdomain based on current literature
Interface between microdomain and cytosol not fully characterized	Assumed PopZ IDRs are extended to bind soluble clients at the interface between microdomain and cytosol
Organization of membrane clients within the membrane is not fully characterized	Assumed uniform, random distribution of membrane-bound clients

microdomain? What is the arrangement of scaffolding proteins inside the condensate and how do they contribute to the arrangement of PopZ molecules? Is the ParB/*parS* interface with PopZ structurally and functionally different from the rest of microdomain? Similarly, is the interface between PopZ and the membrane different from the inner region? This illustration provides a visual conception for each of these questions, with the goal of helping researchers build a mental model of the system for hypothesis generation and further experimentation.

Research on cellular condensates is in a period of exponential growth, with many new examples being continually discovered. As is often true in new fields of

inquiry, information is still fragmentary for many of these systems. The PopZ condensate is among the best studied of condensates, reaching a level where this type of integrative conception is possible without requiring an excessive level of artistic license. Looking forward, we expect that a similar approach will be applicable to many cellular systems. It is becoming apparent that they share many common features, being built around multivalent biomolecules like PopZ that include flexible intrinsically disordered segments in addition to folded regions to promote self-association and interaction with client molecules.

3.3 | Applications

The illustration is intended for general use in dissemination and outreach. For example, we have presented it as part of our professional presentations, such as the workshop “Re-imagining a cellular space occupied by condensates” (October 2022, Salt Lake City, Utah). To promote widespread use, a full-size tif file is freely available through a Creative Commons license at PDB-101, the outreach portal for the RCSB Protein Data Bank (pdb101.rcsb.org) for use in presentations, lessons, and display in laboratories.

4 | PROSPECTS

As mentioned in the introduction, we are increasingly using these types of illustrations at the beginning of large-scale mesoscale modeling projects, as an approachable way to gather and curate information and identify key questions that could be addressed with full 3D modeling. The PopZ microdomain illustration underscores several aspects of the system as we move forward. First, it is one of the most well-studied examples of a cellular condensate, so abundant data is available for many central aspects of the structure. Second, it is a relatively simple system with a manageable number of components, which should be amenable to detailed modeling. The illustration project also identifies several aspects where quantitative information is missing, which could be addressed through further experimental study and modeling. This includes the detailed nature of the PopZ filament, sites of PopZ interaction on client proteins and sites of interaction between neighboring PopZ filaments, the detailed structure of the membrane-bound clients, and the in vivo density of PopZ in the condensate. Detailed 3D models will open the door to study of processes such as the diffusion and capture of clients within the PopZ matrix and the role of membrane-bound clients in the localization of the condensate.

5 | MATERIALS AND METHODS

5.1 | Structural proteome and interactions

Previous studies have shown that PopZ includes Helix 1 near the N-terminus, a central IDR rich in proline and negatively charged amino acids, and three closely spaced helices near the C-terminus involved in oligomerization. These features are apparent in the AlphaFold2 model (AF-Q9A8N4-F1). AlphaFold predictions of the oligomerization domain yielded a parallel three-stranded helical bundle, and docking of two trimers with Haddock (Honorato et al., 2021) yielded a hexamer model with parallel and slightly offset trimers. The width of the hexamer is consistent with the width of PopZ filaments observed in cryoelectron micrographs (Toro-Nahuelpan et al., 2022). The filament is depicted as a speculative head-to-tail arrangement of hexamers, which results in a parallel double helix of trimers.

Soluble client proteins are based on experimental structures as shown in Figure 4. Structures of *Caulobacter* proteins were available for five soluble clients: PDB ID 4fpp (ChpT), 3ctw (RcdA), 6t1f (ParB and DNA), 1w25 (PleD), and 1mb3 (DivK). The ParB/DNA complex is missing the C-terminal domain, which was depicted based on the AlphaFold2 structure (AF-B8GW30-F1). In addition, the structure Spo01 with DNA (PDB ID 4umk) was used to depict the open form of ParB. Homologous proteins were used for three soluble clients, all found using the SWISSMODEL link from the UniProt entry: 6tne (CpdR), 1ys6 (CtrA), and 6t1f (PopA).

Membrane-bound client proteins posed greater challenges. All are based on annotations in UniProt and AlphaFold2 predictions (Figure 5). CckA, PleC, and DivL all contain classic histidine kinase domains, which are dimeric in available crystal structures (5idj and 4q20), so the entire complex was treated as dimeric. CckA is additionally thought to assemble into tetramers (Mann & Shapiro, 2018). PodJ is annotated with a periplasmic Sel1 domain, which may mediate interaction with peptidoglycan, a transmembrane segment, a membrane-proximal IDR, and three closely spaced coiled-coil regions. It was treated as a dimer formed through a speculative long coiled coil. In addition, PodJ is known to be proteolyzed into a shorter form by removing the periplasmic domains (Lawler et al., 2006). Here, we treated all copies as the long form. ZitP was treated as a monomer based on the AlphaFold2 predicted structure.

Interactions with clients and PopZ (Table 2) were through the PopZ Helix 1. Interacting sites on clients are largely uncharacterized, apart from the zinc finger on

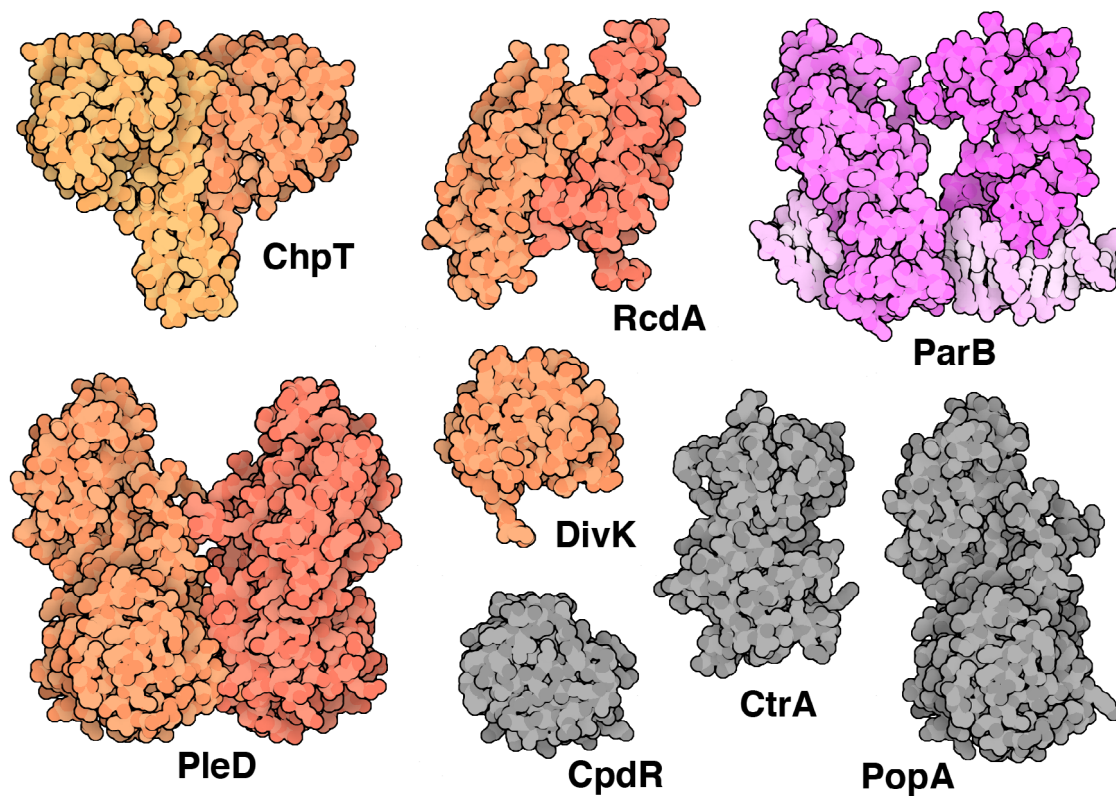


FIGURE 4 Experimental structures of soluble clients. Five structures are *Caulobacter* proteins (shown in color), and three are structures from related organisms or a homologous molecule in *Caulobacter* (shown in gray).

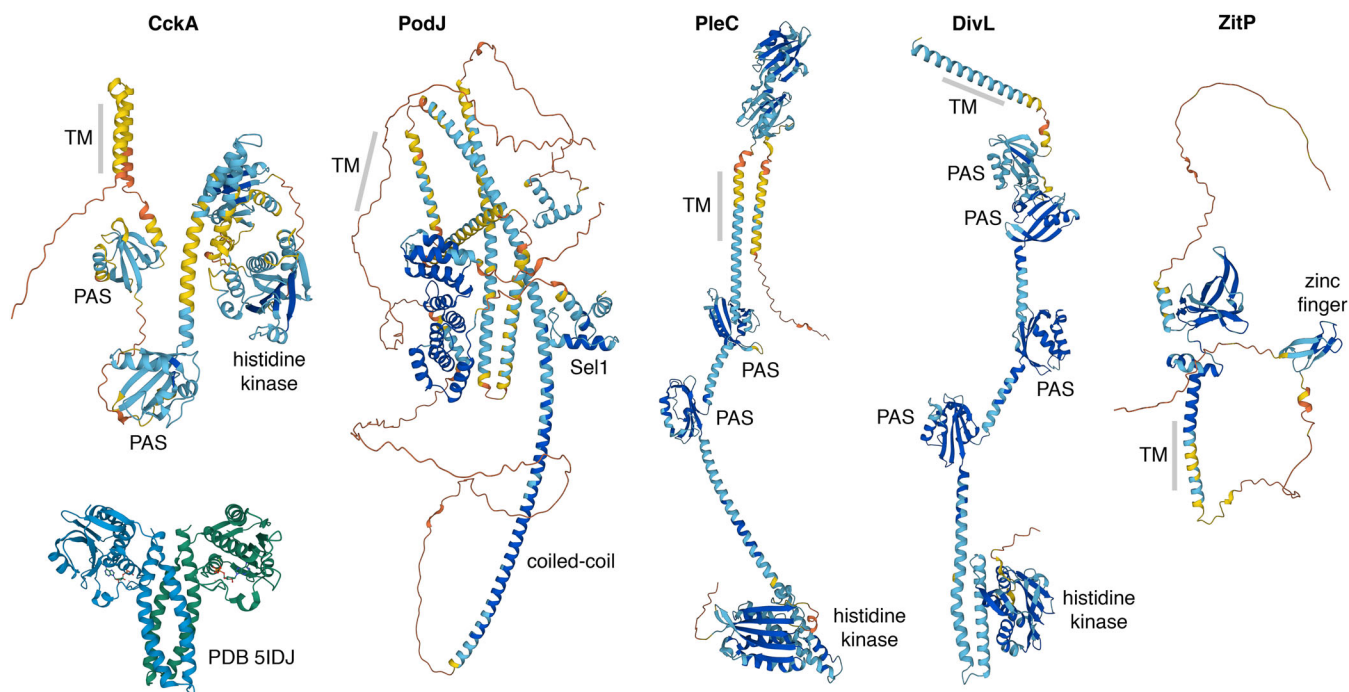


FIGURE 5 AlphaFold2 structures of membrane clients. Structures are colored with the standard scheme, with regions of high confidence in blue and regions of low confidence in yellow and red. The experimental structure of the histidine kinase domain of CckA is shown at lower left for comparison.

ZitP (Bergé et al., 2016) and were depicted in speculative locations.

Structures for cytoplasmic and cell wall proteins were taken largely from a previous illustration of *Escherichia coli* (doi: 10.2210/rcsb_pdb/goodsell-gallery-028). Each protein was confirmed at UniProt to ensure presence in the *Caulobacter* genome. Differences with *E. coli* include absence of porins and lipoprotein LPP in the outer membrane and presence of many TonB-linked transport complexes that span the cell wall. Specific proteins that are depicted were chosen by: (1) first choosing molecules from the 150 most abundant proteins in the ribosome profiling study (Schrader et al., 2016) and (2) filling remaining spaces with proteins from the *E. coli* illustration after verification for presence in the *Caulobacter* genome. The flagellar motor is based on structures from cryoelectron microscopy (Rossmann et al., 2020) and the S-layer is taken from PDB entries 5n97 and 6t72.

5.2 | Abundances

Relative copy numbers for microdomain proteins were obtained from ribosome profiling (Schrader et al., 2016), and the fraction of each protein that is found in the microdomain was estimated from fluorescence microscopy from multiple sources (see references in Table 1). To get absolute numbers for each molecule, we assumed that the microdomain was a sphere of radius 60 nm, and that the overall concentration is equivalent to the protein density in typical bacterial cytoplasm, 0.22 g/mL (bionumbers.hms.harvard.edu/bionumber.aspx?id=107695; Cayley et al., 1991). A total mass was calculated from the copy numbers, fractions, and molecular weights of microdomain proteins, revealing that these numbers needed to be divided roughly by a factor of 3 to yield an acceptable density. We then calculated the number of molecules depicted in the illustration by assuming that the foreground layer represented a central slice through this spherical condensate with a thickness of 10 nm.

5.3 | Ultrastructure

The ultrastructure depicted in the painting is based on a cryoelectron micrograph (Dahlberg et al., 2020). Features taken from this micrograph include the spacing of membranes and S-layer, location of chemosensory array relative to the microdomain, and distribution of ribosomes excluded by the microdomain. Size and spacing of PopZ filaments is based on micrographs (Toro-Nahuelpan et al., 2022).

5.4 | Illustration methods

The illustration was rendered as described previously (Goodsell, 2016). Briefly, style sheets for individual molecules were developed for all molecules and used to create a full sketch of foreground molecules, adding assemblies with long-range coherence first (PopZ filament core, nucleoid, S-layer, membranes, etc.), followed by large molecular assemblies (ribosomes, PopZ IDR), and finally filling remaining spaces with soluble components. The illustration is rendered in watercolor and ink using traditional color washes, starting with foreground and adding background molecules extemporaneously.

AUTHOR CONTRIBUTIONS

David S. Goodsell: Conceptualization (equal); data curation (equal); funding acquisition (equal); investigation (equal); methodology (equal); software (equal); visualization (equal); writing – original draft (equal); writing – review and editing (equal). **Keren Lasker:** Conceptualization (equal); data curation (equal); funding acquisition (equal); investigation (equal); methodology (equal); software (equal); visualization (equal); writing – original draft (equal); writing – review and editing (equal).

ACKNOWLEDGMENTS

This illustration would not have been possible without decades of dedicated work from the *Caulobacter* community, and we acknowledge all *Caulobacter* labs across the globe. We thank Seth Childers, Peter Chien, and Jared Schrader for discussions on specific details included in this project. We thank members of the Lasker lab, in particular Daniel Scholl and Asma Khan, for sharing data relating to the structure and assembly pathway of the PopZ condensate. We also thank Steven Boeynaems and Alex Holehouse for continued collaboration of the PopZ condensate biophysics and function. This work was supported by grant GM120604 from the National Institutes of Health and the RCSB Protein Data Bank (National Science Foundation DBI-1832184, National Institutes of Health GM133198, and US Department of Energy DE-SC0019749).

CONFLICT OF INTEREST STATEMENT

The authors declare no conflicts of interest.

DATA AVAILABILITY STATEMENT

Included in the article: "A full-size digital file and key are available for unrestricted use at PDB-101, the outreach portal of the RCSB Protein Data Bank at doi: 10.2210/rcsb_pdb/goodsell-gallery-046."

ORCID

David S. Goodsell  <https://orcid.org/0000-0002-5932-2130>

Keren Lasker  <https://orcid.org/0000-0002-5480-4173>

REFERENCES

- Abel S, Bucher T, Nicollier M, et al. Bi-modal distribution of the second messenger c-di-GMP controls cell fate and asymmetry during the *Caulobacter* cell cycle. *PLoS Genet.* 2013;9(9):e1003744. <https://doi.org/10.1371/journal.pgen.1003744>
- Abeles AL, Friedman SA, Austin SJ. Partition of unit-copy miniplasmids to daughter cells. *J Mol Biol.* 1985;185(2):261–72. [https://doi.org/10.1016/0022-2836\(85\)90402-4](https://doi.org/10.1016/0022-2836(85)90402-4)
- Aldridge P, Paul R, Goymer P, Rainey P, Jenal U. Role of the GGDEF regulator PleD in polar development of *Caulobacter crescentus*: PleD control of polar development. *Mol Microbiol.* 2003;47(6):1695–708. <https://doi.org/10.1046/j.1365-2958.2003.03401.x>
- Angelastro PS, Sliusarenko O, Jacobs-Wagner C. Polar localization of the CckA histidine kinase and cell cycle periodicity of the essential master regulator CtrA in *Caulobacter crescentus*. *J Bacteriol.* 2010;192(2):539–52. <https://doi.org/10.1128/JB.00985-09>
- Antar H, Soh YM, Zamuner S, Bock FP, Anchimiuk A, Rios PL, et al. Relief of ParB autoinhibition by *parS* DNA catalysis and recycling of ParB by CTP hydrolysis promote bacterial centromere assembly. *Sci Adv.* 2021;7(41):eabj2854. <https://doi.org/10.1126/sciadv.abj2854>
- Ardissone S, Viollier PH. Interplay between flagellation and cell cycle control in *Caulobacter*. *Curr Opin Microbiol.* 2015;28:83–92. <https://doi.org/10.1016/j.mib.2015.08.012>
- Austin S, Abeles A. Partition of unit-copy miniplasmids to daughter cells. *J Mol Biol.* 1983;169(2):373–87. [https://doi.org/10.1016/S0022-2836\(83\)80056-4](https://doi.org/10.1016/S0022-2836(83)80056-4)
- Banani SF, Lee HO, Hyman AA, Rosen MK. Biomolecular condensates: organizers of cellular biochemistry. *Nat Rev Mol Cell Biol.* 2017;18(5):285–98. <https://doi.org/10.1038/nrm.2017.7>
- Bergé M, Campagne S, Mignolet J, Holden S, Théraulaz L, Manley S, et al. Modularity and determinants of a (bi-)polarization control system from free-living and obligate intracellular bacteria. *Elife.* 2016;5:e20640. <https://doi.org/10.7554/eLife.20640>
- Biondi EG, Reisinger SJ, Skerker JM, Arif M, Perchuk BS, Ryan KR, et al. Regulation of the bacterial cell cycle by an integrated genetic circuit. *Nature.* 2006;444(7121):899–904. <https://doi.org/10.1038/nature05321>
- Blair JA, Xu Q, Childers WS, Mathews II, Kern JW, Eckart M, et al. Branched signal wiring of an essential bacterial cell-cycle phosphotransfer protein. *Structure.* 2013;21(9):1590–601. <https://doi.org/10.1016/j.str.2013.06.024>
- Böhm K, Giacomelli G, Schmidt A, Imhof A, Koszul R, Marbouty M, et al. Chromosome organization by a conserved condensin-ParB system in the actinobacterium *Corynebacterium glutamicum*. *Nat Commun.* 2020;11(1):1485. <https://doi.org/10.1038/s41467-020-15238-4>
- Bowman GR, Comolli LR, Gaietta GM, Fero M, Hong SH, Jones Y, et al. *Caulobacter* PopZ forms a polar subdomain dictating sequential changes in pole composition and function. *Mol Microbiol.* 2010;76(1):173–89. <https://doi.org/10.1111/j.1365-2958.2010.07088.x>
- Bowman GR, Comolli LR, Zhu J, Eckart M, Koenig M, Downing KH, et al. A polymeric protein anchors the chromosomal origin/ParB complex at a bacterial cell pole. *Cell.* 2008;134(6):945–55. <https://doi.org/10.1016/j.cell.2008.07.015>
- Bowman GR, Perez AM, Ptacin JL, Ighodaro E, Folta-Stogniew E, Comolli LR, et al. Oligomerization and higher-order assembly contribute to sub-cellular localization of a bacterial scaffold: mutational analysis of PopZ. *Mol Microbiol.* 2013;90(4):776–95. <https://doi.org/10.1111/mmi.12398>
- Breier AM, Grossman AD. Whole-genome analysis of the chromosome partitioning and sporulation protein Spo0J (ParB) reveals spreading and origin-distal sites on the *Bacillus subtilis* chromosome. *Mol Microbiol.* 2007;64(3):703–18. <https://doi.org/10.1111/j.1365-2958.2007.05690.x>
- Cayley S, Lewis BA, Guttman HJ, Record MT. Characterization of the cytoplasm of *Escherichia coli* K-12 as a function of external osmolarity. *J Mol Biol.* 1991;222(2):281–300. [https://doi.org/10.1016/0022-2836\(91\)90212-O](https://doi.org/10.1016/0022-2836(91)90212-O)
- Chen YE, Tsokos CG, Biondi EG, Perchuk BS, Laub MT. Dynamics of two phosphorelays controlling cell cycle progression in *Caulobacter crescentus*. *J Bacteriol.* 2009;191(24):7417–29. <https://doi.org/10.1128/JB.00992-09>
- Childers WS, Xu Q, Mann TH, et al. Cell fate regulation governed by a repurposed bacterial histidine kinase. *PLoS Biol.* 2014;12(10):e1001979. <https://doi.org/10.1371/journal.pbio.1001979>
- Christen M, Kulasekara HD, Christen B, Kulasekara BR, Hoffman LR, Miller SI. Asymmetrical distribution of the second messenger c-di-GMP upon bacterial cell division. *Science.* 2010;328(5983):1295–7. <https://doi.org/10.1126/science.1188658>
- Curtis PD, Brun YV. Getting in the loop: regulation of development in *Caulobacter crescentus*. *Microbiol Mol Biol Rev.* 2010;74:13–41.
- Curtis PD, Quardokus EM, Lawler ML, Guo X, Klein D, Chen JC, et al. The scaffolding and signalling functions of a localization factor impact polar development: analysis of PodJ functions. *Mol Microbiol.* 2012;84(4):712–35. <https://doi.org/10.1111/j.1365-2958.2012.08055.x>
- Dahlberg PD, Saurabh S, Sartor AM, Wang J, Mitchell PG, Chiu W, et al. Cryogenic single-molecule fluorescence annotations for electron tomography reveal in situ organization of key proteins in *Caulobacter*. *Proc Natl Acad Sci U S A.* 2020;117(25):13937–44. <https://doi.org/10.1073/pnas.2001849117>
- Domian IJ, Quon KC, Shapiro L. Cell type-specific phosphorylation and proteolysis of a transcriptional regulator controls the G1-to-S transition in a bacterial cell cycle. *Cell.* 1997;90(3):415–24. [https://doi.org/10.1016/S0092-8674\(00\)80502-4](https://doi.org/10.1016/S0092-8674(00)80502-4)
- Duerig A, Abel S, Folcher M, Nicollier M, Schwede T, Amiot N, et al. Second messenger-mediated spatiotemporal control of protein degradation regulates bacterial cell cycle progression. *Genes Dev.* 2009;23(1):93–104. <https://doi.org/10.1101/gad.502409>
- Easter J, Gober JW. ParB-stimulated nucleotide exchange regulates a switch in functionally distinct ParA activities. *Mol Cell.* 2002;10(2):427–34. [https://doi.org/10.1016/S1097-2765\(02\)00594-4](https://doi.org/10.1016/S1097-2765(02)00594-4)
- Ebersbach G, Briegel A, Jensen GJ, Jacobs-Wagner C. A self-associating protein critical for chromosome attachment, division, and polar organization in *Caulobacter*. *Cell.* 2008;134(6):956–68. <https://doi.org/10.1016/j.cell.2008.07.016>

- Fatima NI, Fazili KM, Bhat NH. Proteolysis dependent cell cycle regulation in *Caulobacter crescentus*. *Cell Div*. 2022;17(1):3. <https://doi.org/10.1186/s13008-022-00078-z>
- Figge RM, Easter J, Gober JW. Productive interaction between the chromosome partitioning proteins, ParA and ParB, is required for the progression of the cell cycle in *Caulobacter crescentus*: dominant-negative ParB alleles. *Mol Microbiol*. 2003;47(5):1225–37. <https://doi.org/10.1046/j.1365-2958.2003.03367.x>
- Frandi A, Collier J. Multilayered control of chromosome replication in *Caulobacter crescentus*. *Biochem Soc Trans*. 2019;47(1):187–96. <https://doi.org/10.1042/BST20180460>
- Gahlmann A, Ptacin JL, Grover G, Quirin S, von Diezmann L, Lee MK, et al. Quantitative multicolor subdiffraction imaging of bacterial protein ultrastructures in three dimensions. *Nano Lett*. 2013;13(3):987–93. <https://doi.org/10.1021/nl304071h>
- Gewin V. How to forge a productive science-art collaboration. *Nature*. 2021;580:515–8.
- Goodsell D. Cellular landscapes in watercolor. *J Biocommun*. 2016;40(1):22–6. <https://doi.org/10.5210/jbc.v40i1.6627>
- Goodsell DS. Inside a living cell. *Trends Biochem Sci*. 1991;16(6):203–6. [https://doi.org/10.1016/0968-0004\(91\)90083-8](https://doi.org/10.1016/0968-0004(91)90083-8)
- Goodsell DS. *Escherichia coli*. *Biochem Mol Biol Educ*. 2009;37(6):325–32. <https://doi.org/10.1002/bmb.20345>
- Goodsell DS. Art as a tool for science. *Nat Struct Mol Biol*. 2021;28(5):402–3. <https://doi.org/10.1038/s41594-021-00587-5>
- Goodsell DS. Integrative illustration of a JCVI-syn3A minimal cell. *J Integr Bioinform*. 2022;19(2):20220013. <https://doi.org/10.1515/jib-2022-0013>
- Gora KG, Cantin A, Wohlever M, Joshi KK, Perchuk BS, Chien P, et al. Regulated proteolysis of a transcription factor complex is critical to cell cycle progression in *Caulobacter crescentus*: cell cycle regulated proteolysis in *Caulobacter*. *Mol Microbiol*. 2013;87(6):1277–89. <https://doi.org/10.1111/mmi.12166>
- Govers SK, Jacobs-Wagner C. *Caulobacter crescentus*: model system extraordinaire. *Curr Biol*. 2020;30:R1151–8.
- Guo MS, Haakonsen DL, Zeng W, Schumacher MA, Laub MT. A bacterial chromosome structuring protein binds overtwisted DNA to stimulate type II topoisomerases and enable DNA replication. *Cell*. 2018;175(2):583–597.e23. <https://doi.org/10.1016/j.cell.2018.08.029>
- Guzzo M, Sanderlin AG, Castro LK, Laub MT. Activation of a signaling pathway by the physical translocation of a chromosome. *Dev Cell*. 2021;56(15):2145–2159.e7. <https://doi.org/10.1016/j.devcel.2021.06.014>
- Hecht GB, Lane T, Ohta N, Sommer JM, Newton A. An essential single domain response regulator required for normal cell division and differentiation in *Caulobacter crescentus*. *EMBO J*. 1995;14(16):3915–24. <https://doi.org/10.1002/j.1460-2075.1995.tb00063.x>
- Hecht GB, Newton A. Identification of a novel response regulator required for the swarmer-to-stalked-cell transition in *Caulobacter crescentus*. *J Bacteriol*. 1995;177(21):6223–9. <https://doi.org/10.1128/jb.177.21.6223-6229.1995>
- Hinz AJ, Larson DE, Smith CS, Brun YV. The *Caulobacter crescentus* polar organelle development protein PodJ is differentially localized and is required for polar targeting of the PleC development regulator: differential localization of PodJ. *Mol Microbiol*. 2003;47(4):929–41. <https://doi.org/10.1046/j.1365-2958.2003.03349.x>
- Holmes JA, Follett SE, Wang H, Meadows CP, Varga K, Bowman GR. *Caulobacter* PopZ forms an intrinsically disordered hub in organizing bacterial cell poles. *Proc Natl Acad Sci U S A*. 2016;113(44):12490–5. <https://doi.org/10.1073/pnas.1602380113>
- Honorato RV, Koukos PI, Jiménez-García B, Tsaregorodtsev A, Verlati M, Giachetti A, et al. Structural biology in the clouds: the WeNMR-EOSC ecosystem. *Front Mol Biosci*. 2021;8:729513. <https://doi.org/10.3389/fmolb.2021.729513>
- Iniesta AA, McGrath PT, Reisenauer A, McAdams HH, Shapiro L. A phospho-signaling pathway controls the localization and activity of a protease complex critical for bacterial cell cycle progression. *Proc Natl Acad Sci*. 2006;103(29):10935–40. <https://doi.org/10.1073/pnas.0604554103>
- Iniesta AA, Shapiro L. A bacterial control circuit integrates polar localization and proteolysis of key regulatory proteins with a phospho-signaling cascade. *Proc Natl Acad Sci U S A*. 2008;105(43):16602–7. <https://doi.org/10.1073/pnas.0808807105>
- Jacobs C, Domian IJ, Maddock JR, Shapiro L. Cell cycle-dependent polar localization of an essential bacterial histidine kinase that controls DNA replication and cell division. *Cell*. 1999;97(1):111–20. [https://doi.org/10.1016/S0092-8674\(00\)80719-9](https://doi.org/10.1016/S0092-8674(00)80719-9)
- Jacobs C, Hung D, Shapiro L. Dynamic localization of a cytoplasmic signal transduction response regulator controls morphogenesis during the *Caulobacter* cell cycle. *Proc Natl Acad Sci U S A*. 2001;98(7):4095–100. <https://doi.org/10.1073/pnas.051609998>
- Jalal ASB, Le TBK. Bacterial chromosome segregation by the ParABS system. *Open Biol*. 2020;10(6):200097. <https://doi.org/10.1098/rsob.200097>
- Jensen RB, Shapiro L. The *Caulobacter crescentus* smc gene is required for cell cycle progression and chromosome segregation. *Proc Natl Acad Sci U S A*. 1999;96(19):10661–6. <https://doi.org/10.1073/pnas.96.19.10661>
- Joshi KK, Bergé M, Radhakrishnan SK, Viollier PH, Chien P. An adaptor hierarchy regulates proteolysis during a bacterial cell cycle. *Cell*. 2015;163(2):419–31. <https://doi.org/10.1016/j.cell.2015.09.030>
- Joshi KK, Chien P. Regulated proteolysis in bacteria: *Caulobacter*. *Annu Rev Genet*. 2016;50(1):423–45. <https://doi.org/10.1146/annurev-genet-120215-035235>
- Jumper J, Evans R, Pritzel A, Green T, Figurnov M, Ronneberger O, et al. Highly accurate protein structure prediction with AlphaFold. *Nature*. 2021;596:583–9. <https://doi.org/10.1038/s41586-021-03819-2>
- Lagage V, Boccard F, Vallet-Gely I. Regional control of chromosome segregation in *Pseudomonas aeruginosa*. *PLOS Genet*. 2016;12(11):e1006428. <https://doi.org/10.1371/journal.pgen.1006428>
- Laloux G, Jacobs-Wagner C. Spatiotemporal control of PopZ localization through cell cycle-coupled multimerization. *J Cell Biol*. 2013;201:827–41.
- Lam H, Matroule JY, Jacobs-Wagner C. The asymmetric spatial distribution of bacterial signal transduction proteins coordinates cell cycle events. *Dev Cell*. 2003;5(1):149–59. [https://doi.org/10.1016/S1534-5807\(03\)00191-6](https://doi.org/10.1016/S1534-5807(03)00191-6)
- Lasker K, Boeynaems S, Lam V, Scholl D, Stainton E, Briner A, et al. The material properties of a bacterial-derived biomolecular condensate tune biological function in natural and synthetic systems. *Nat Commun*. 2022;13(1):5643. <https://doi.org/10.1038/s41467-022-33221-z>

- Lasker K, Mann TH, Shapiro L. An intracellular compass spatially coordinates cell cycle modules in *Caulobacter crescentus*. *Curr Opin Microbiol*. 2016;33:131–9. <https://doi.org/10.1016/j.mib.2016.06.007>
- Lasker K, von Diezmann L, Zhou X, Ahrens DG, Mann TH, Moerner WE, et al. Selective sequestration of signalling proteins in a membraneless organelle reinforces the spatial regulation of asymmetry in *Caulobacter crescentus*. *Nat Microbiol*. 2020;5(3):418–29. <https://doi.org/10.1038/s41564-019-0647-7>
- Laub MT, Chen SL, Shapiro L, McAdams HH. Genes directly controlled by CtrA, a master regulator of the *Caulobacter* cell cycle. *Proc Natl Acad Sci*. 2002;99(7):4632–7. <https://doi.org/10.1073/pnas.062065699>
- Lawler ML, Larson DE, Hinz AJ, Klein D, Brun YV. Dissection of functional domains of the polar localization factor PodJ in *Caulobacter crescentus*. *Mol Microbiol*. 2006;59(1):301–16. <https://doi.org/10.1111/j.1365-2958.2005.04935.x>
- Leonard TA, Butler PJ, Löwe J. Bacterial chromosome segregation: structure and DNA binding of the Soj dimer? A conserved biological switch. *EMBO J*. 2005;24(2):270–82. <https://doi.org/10.1038/sj.emboj.7600530>
- Livny J, Yamaichi Y, Waldor MK. Distribution of centromere-like *parS* sites in bacteria: insights from comparative genomics. *J Bacteriol*. 2007;189(23):8693–703. <https://doi.org/10.1128/JB.01239-07>
- Lori C, Ozaki S, Steiner S, Böhm R, Abel S, Dubey BN, et al. Cyclic di-GMP acts as a cell cycle oscillator to drive chromosome replication. *Nature*. 2015;523(7559):236–9. <https://doi.org/10.1038/nature14473>
- Mann TH, Seth Childers W, Blair JA, Eckart MR, Shapiro L. A cell cycle kinase with tandem sensory PAS domains integrates cell fate cues. *Nat Commun*. 2016;7(1):11454. <https://doi.org/10.1038/ncomms11454>
- Mann TH, Shapiro L. Integration of cell cycle signals by multi-PAS domain kinases. *Proc Natl Acad Sci U S A*. 2018;115(30):E7166–73. <https://doi.org/10.1073/pnas.1808543115>
- Maritan M, Autin L, Karr J, Covert MW, Olson AJ, Goodsell DS. Building structural models of a whole mycoplasma cell. *J Mol Biol*. 2022;434(2):167351. <https://doi.org/10.1016/j.jmb.2021.167351>
- Matroule JY, Lam H, Burnette DT, Jacobs-Wagner C. Cytokinesis monitoring during development. *Cell*. 2004;118(5):579–90. <https://doi.org/10.1016/j.cell.2004.08.019>
- McGrath PT, Iniesta AA, Ryan KR, Shapiro L, McAdams HH. A dynamically localized protease complex and a polar specificity factor control a cell cycle master regulator. *Cell*. 2006;124(3):535–47. <https://doi.org/10.1016/j.cell.2005.12.033>
- Mignolet J, Panis G, Viollier PH. More than a tad: spatiotemporal control of *Caulobacter* pili. *Curr Opin Microbiol*. 2018;42:79–86. <https://doi.org/10.1016/j.mib.2017.10.017>
- Mohl DA, Easter J, Gober JW. The chromosome partitioning protein, ParB, is required for cytokinesis in *Caulobacter crescentus*: ParB is required for cell division in *Caulobacter*. *Mol Microbiol*. 2008;42(3):741–55. <https://doi.org/10.1046/j.1365-2958.2001.02643.x>
- Mori H, Kondo A, Ohshima A, Ogura T, Hiraga S. Structure and function of the F plasmid genes essential for partitioning. *J Mol Biol*. 1986;192(1):1–15. [https://doi.org/10.1016/0022-2836\(86\)90459-6](https://doi.org/10.1016/0022-2836(86)90459-6)
- Nordyke CT, Ahmed YM, Puterbaugh RZ, Bowman GR, Varga K. Intrinsically disordered bacterial polar organizing protein Z, PopZ, interacts with protein binding partners through an N-terminal molecular recognition feature. *J Mol Biol*. 2020;432(23):6092–107. <https://doi.org/10.1016/j.jmb.2020.09.020>
- Paul R, Weiser S, Amiot NC, Chan C, Schirmer T, Giese B, et al. Cell cycle-dependent dynamic localization of a bacterial response regulator with a novel di-guanylate cyclase output domain. *Genes Dev*. 2004;18(6):715–27. <https://doi.org/10.1101/gad.289504>
- Posey AE, Holehouse AS, Pappu RV. Phase separation of intrinsically disordered proteins. *Methods Enzymol*. 2018;611:1–30. <https://doi.org/10.1016/bs.mie.2018.09.035>
- Ptacin JL, Gahlmann A, Bowman GR, Perez AM, von Diezmann L, Eckart MR, et al. Bacterial scaffold directs pole-specific centromere segregation. *Proc Natl Acad Sci U S A*. 2014;111(19):E2046–55. <https://doi.org/10.1073/pnas.1405188111>
- Ptacin JL, Lee SF, Garner EC, Toro E, Eckart M, Comolli LR, et al. A spindle-like apparatus guides bacterial chromosome segregation. *Nat Cell Biol*. 2010;12(8):791–8. <https://doi.org/10.1038/ncb2083>
- Quon KC, Yang B, Domian IJ, Shapiro L, Marczyński GT. Negative control of bacterial DNA replication by a cell cycle regulatory protein that binds at the chromosome origin. *Proc Natl Acad Sci U S A*. 1998;95(1):120–5. <https://doi.org/10.1073/pnas.95.1.120>
- Reisinger SJ, Huntwork S, Viollier PH, Ryan KR. DivL performs critical cell cycle functions in *Caulobacter crescentus* independent of kinase activity. *J Bacteriol*. 2007;189(22):8308–20. <https://doi.org/10.1128/JB.00868-07>
- Root-Bernstein B, Siler T, Brown A, Snelson K. ArtScience: integrative collaboration to create a sustainable future. *Leonardo*. 2011;44(3):192–2. https://doi.org/10.1162/LEON_e_00161
- Rossmann FM, Hug I, Sangermani M, Jenal U, Beeby M. In situ structure of the *Caulobacter crescentus* flagellar motor and visualization of binding of a CheY-homolog. *Mol Microbiol*. 2020;114(3):443–53. <https://doi.org/10.1111/mmi.14525>
- Ryan KR, Huntwork S, Shapiro L. Recruitment of a cytoplasmic response regulator to the cell pole is linked to its cell cycle-regulated proteolysis. *Proc Natl Acad Sci*. 2004;101(19):7415–20. <https://doi.org/10.1073/pnas.0402153101>
- Schrader JM, Li GW, Childers WS, Perez AM, Weissman JS, Shapiro L, et al. Dynamic translation regulation in *Caulobacter* cell cycle control. *Proc Natl Acad Sci U S A*. 2016;113(44):E6859–67. <https://doi.org/10.1073/pnas.1614795113>
- Schroeder K, Jonas K. The protein quality control network in *Caulobacter crescentus*. *Front Mol Biosci*. 2021;8:682967. <https://doi.org/10.3389/fmolb.2021.682967>
- Shin Y, Brangwynne CP. Liquid phase condensation in cell physiology and disease. *Science*. 2017;357(6357):eaaf4382. <https://doi.org/10.1126/science.aaf4382>
- Smith SC, Joshi KK, Zik JJ, Trinh K, Kamajaya A, Chien P, et al. Cell cycle-dependent adaptor complex for ClpXP-mediated proteolysis directly integrates phosphorylation and second messenger signals. *Proc Natl Acad Sci U S A*. 2014;111(39):14229–34. <https://doi.org/10.1073/pnas.1407862111>
- Toro-Nahuelpan M, Plitzko JM, Schüler D, Pfeiffer D. In vivo architecture of the polar organizing protein Z (PopZ) meshwork in the Alphaproteobacteria *Magnetospirillum gryphiswaldense* and

- Caulobacter crescentus*. J Mol Biol. 2022;434(5):167423. <https://doi.org/10.1016/j.jmb.2021.167423>
- Tran NT, Laub MT, Le TBK. SMC progressively aligns chromosomal arms in *Caulobacter crescentus* but is antagonized by convergent transcription. Cell Rep. 2017;20(9):2057–71. <https://doi.org/10.1016/j.celrep.2017.08.026>
- Tsokos CG, Laub MT. Polarity and cell fate asymmetry in *Caulobacter crescentus*. Curr Opin Microbiol. 2012;15(6):744–50. <https://doi.org/10.1016/j.mib.2012.10.011>
- Tsokos CG, Perchuk BS, Laub MT. A dynamic complex of signaling proteins uses polar localization to regulate cell-fate asymmetry in *Caulobacter crescentus*. Dev Cell. 2011;20(3):329–41. <https://doi.org/10.1016/j.devcel.2011.01.007>
- Viollier PH, Sternheim N, Shapiro L. Identification of a localization factor for the polar positioning of bacterial structural and regulatory proteins. Proc Natl Acad Sci U S A. 2002;99(21):13831–6. <https://doi.org/10.1073/pnas.182411999>
- Wang J, Moerner WE, Shapiro L. A localized adaptor protein performs distinct functions at the *Caulobacter* cell poles. Proc Natl Acad Sci U S A. 2021;118(13):e2024705118. <https://doi.org/10.1073/pnas.2024705118>
- Wheeler RT, Shapiro L. Differential localization of two histidine kinases controlling bacterial cell differentiation. Mol Cell. 1999;4(5):683–94. [https://doi.org/10.1016/S1097-2765\(00\)80379-2](https://doi.org/10.1016/S1097-2765(00)80379-2)
- Zhang C, Zhao W, Duvall SW, Kowallis KA, Childers WS. Regulation of the activity of the bacterial histidine kinase PleC by the scaffolding protein PodJ. J Biol Chem. 2022;298(4):101683. <https://doi.org/10.1016/j.jbc.2022.101683>
- Zhao W, Duvall SW, Kowallis KA, Tomares DT, Petitjean HN, Childers WS. A circuit of protein-protein regulatory interactions enables polarity establishment in a bacterium. Microbiology. 2018, bioRxiv 503250. <https://doi.org/10.1101/503250>
- Zhu L, Goyal Y. Art and science: intersections of art and science through time and paths forward. EMBO Rep. 2019;20(2):e47061. <https://doi.org/10.15252/embr.201847061>
- Zik JJ, Ryan KR. Cell cycle signal transduction and proteolysis in *Caulobacter*. In: Biondi E, editor. Cell cycle regulation and development in Alphaproteobacteria. Cham, Switzerland: Springer International Publishing; 2022. p. 65–100. https://doi.org/10.1007/978-3-030-90621-4_3

How to cite this article: Goodsell DS, Lasker K. Integrative visualization of the molecular structure of a cellular microdomain. Protein Science. 2023; 32(3):e4577. <https://doi.org/10.1002/pro.4577>